ELSEVIER

Polymer 44 (2003) 2005–2013

polymer

www.elsevier.com/locate/polymer

In situ graft copolymerisation: salami morphologies in PMMA/EP blends: part I

J.U. Schierholz, G.P. Hellmann*

Deutsches Kunststoff-Institut, Schlossgartenstrasse 6, D-64289 Darmstadt, Germany

Received 19 July 2002; received in revised form 18 November 2002; accepted 18 November 2002

Abstract

Rubber-modified polystyrene (PS) owes its impact resistance to a morphology of salami domains: in the PS matrix, polybutadiene (PB) domains are dispersed that, in turn, are strongly filled with PS subdomains. This unique structure is created in situ as styrene is polymerized in PB/styrene solutions. The salami domains are built up by graft copolymer chains PB-*g*-PS. It was suggested previously that these domains assume their characteristic architecture because strongly grafted chains stabilize them on the outside while weakly grafted chains provide their internal substructure. This model is extended in this paper that deals with the polymerisation of methylmethacrylate (MMA) in EP/MMA solutions of a poly(ethylene-*co*-propylene) copolymer (EP). Intermediate and final products were characterized by ^{1}H NMR spectroscopy, transmission electron microscopy, two-dimensional chromatography and statistical calculations, with a focus on the pivotal stage of phase inversion during the polymerisation where the salami domains are born.

Keywords: Radical polymerisation; Copolymers; Nanophases

1. Introduction

Commercial high-impact polystyrene (HIPS) owes its toughness to the unique *salami domains* of polybutadiene (BR) shown in Fig. 1 [1–6]. With their many PS subdomains, surrounded by BR lamellae, they look spectacular. In industry, the size and architecture of these salami domains have been optimized for control of multi-crazing [7–9] in the PS matrix and nanocavitation [10,11] of the BR lamellae. It is astonishing that these domains are formed more or less automatically: they are created in situ as styrene is polymerized in solutions of BR in styrene. At the end of the polymerisation, the salami domains are there and the HIPS is ready for the market.

The chemistry is shown in Fig. 2, in general terms of two polymers PA and PB. The polymerisation of the monomer B in a mixture PA/B is started by initiator radicals that create radicals on the polymer chains PA as well as on the monomers B. This leads to grafts PB-*g* on PA-*g* chains as well as to free homopolymer chains PB-h. The mechanism is known as *grafting-from* because the PB-*g* grafts grow from the PA-*g* backbones [12–15] (as opposed to *grafting-onto* in polymer–polymer systems [16,17]). The question discussed in this report is why should this polymerisation in BR/styrene solutions lead to domain structures as in Fig. 1?

In HIPS, the pair PA/PB is BR/PS but other combinations of an elastomer (PA) and a thermoplastic (PB) yield salami morphologies as well. This report deals with an ethylene–propylene copolymer (PA = EP) and polymethylmethacrylate (PB = PMMA) [18–21]. First, a model for salami domains, suggested in Ref. [22], is reviewed, then salami morphologies are shown of products from EP/MMA solutions and, finally, the composition of these products is analyzed in various stages of the synthetic process. A second part of this study will be devoted to methods of altering salami morphologies.

2. Chemical conditions for salami domains

Feed solutions PA/B for grafting-from processes (Fig. 2) turn, during the polymerisation, into complex solutions PA-h/PB-h/PA-*g*-PB/B containing the ungrafted polymers PA-h and PB-h and the graft copolymer PA-*g*-PB. To understand the salami architecture (Fig. 1), the ever-changing

* Corresponding author.
E-mail address: ghellmann@dki.tu-darmstadt (G.P. Hellmann).

0032-3861/03/$ - see front matter © 2002 Elsevier Science Ltd. All rights reserved.
PII: S0032-3861(02)00876-5

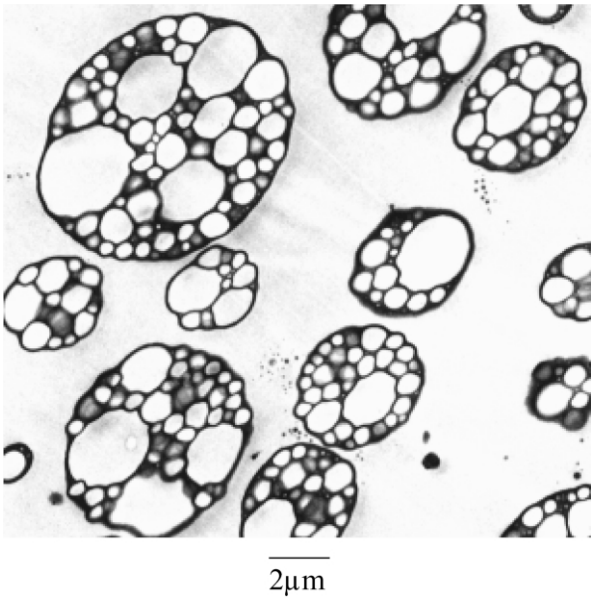

Fig. 1. HIPS: salami domains of polybutadiene (black), filled with polystyrene subdomains (white), in a polystyrene matrix (white).

composition of this polymer mixture must be linked to the corresponding changes in morphology. The following analysis is guided by the model from Ref. [22] which will be extended.

The polymerisation B → PB (without grafting) is shown in Fig. 3 by the arrow 1–5. The feed (1) is a homogeneous solution PA/B which demixes early (2) into coexisting solutions PA/B and PB/B. The PB/B phase is at first dispersed in the matrix of the PA/B phase (m_A) but, as more and more PB is created, the system undergoes, after a cocontinuous stage (cc), a matrix inversion (3) where the PB/B phase takes over the matrix (m_B). All along, the ongoing polymerisation induces the changes in morphology. But the system becomes more and more viscous, in late stages, until stirring becomes finally (4) so inefficient that the solution is practically immobilized so the morphology remains constant up to complete conversion (5).

The composition of such a system is parameterized by the weight ratio R of B and PA in the feed (at $t = 0$), and by the balance π of the polymers PB and PA during the

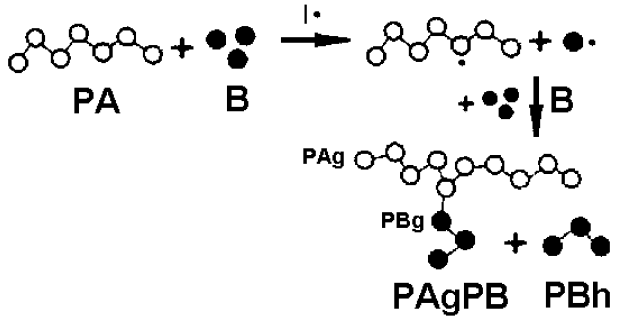

Fig. 2. Grafting-from in a solution PA/B, initiated with radicals I˙.

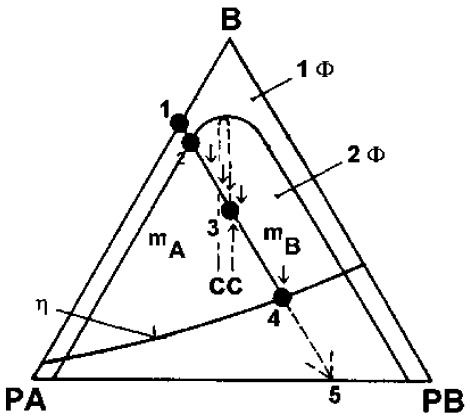

Fig. 3. Polymerisation B → PB (arrows 1–5) in a solution PA/B (point 1): one-phase (1Φ) and two-phase (2Φ) region (sectors: matrix PA (m_A), cocontiuous (cc), matrix PB (m_B)), viscosity limit (η), points for phase separation (2), matrix inversion (3), immobilisation (4) and completion (5), small arrows: stages where the pictures in Fig. 7 were taken.

polymerisation (at $t > 0$):

$$R = \frac{m_B(t=0)}{m_{PA}}, \qquad \pi(t) = \frac{m_{PB}(t)}{m_{PA}} = \left(\frac{w_{PB}}{w_{PA}}\right)(t) \tag{1}$$

The conversion parameter π describes the polymerisation B → PB, varying inside $0 < \pi < R$. The matrix inversion occurs at $\pi \cong 1$ where the weight fractions of PA and PB are approximately equal (conversions in Fig. 3: $\pi = 0$ at (1), $\pi \cong 1$ at (3) and $\pi = R$ at (5)).

When grafting is involved in the polymerisation process, Fig. 3 does not change much. But the matrix inversion at $\pi \cong 1$ becomes an extremely important phenomenon because, 'in this stage, the salami domains are born'.

The composition of a grafting-from mixture PA/PB is shown in Fig. 4, in the stage of matrix inversion ($\pi = 0.92$). In fact, a particular system EP/PMMA is shown that will be discussed later. In Fig. 4a, the weight fractions of the homopolymers PA-h and PB-h and the copolymer PA-g-PB with its subchains PA-g and PB-g are specified together with the molar masses of these components. Fig. 4b shows the distribution of PA chains differing in the number of grafts.

These graphs are based partly on measurements and partly on model calculations. The grafting efficiency can be derived from the weight fractions w_i. It is characterized by fractions $(1 - f_i)$, where the f_i are the homopolymer fractions, and by the composition x of the graft copolymer PA_{1-x}-g-PB_x):

$$f_{PAh} = \frac{w_{PAh}}{w_{PB}}, \qquad f_{PBh} = \frac{w_{PBh}}{w_{PB}}, \qquad x = \frac{w_{PBg}}{w_{PAg}} \tag{2}$$

The number G of PB-g grafts per PA-g backbone results from weight fractions w_i and molar masses M_i (Eq. (A5)):

$$G = \frac{m_{PBg}/m_{PAg}}{M_{PBg}/M_{PAg}} = 1 + (1 - f_{PBh})\frac{M_{PA}}{M_{PB}}\pi \tag{3}$$

All weight fractions w_i can be measured reliably but not all molar masses M_i. Therefore, the experiments alone do not

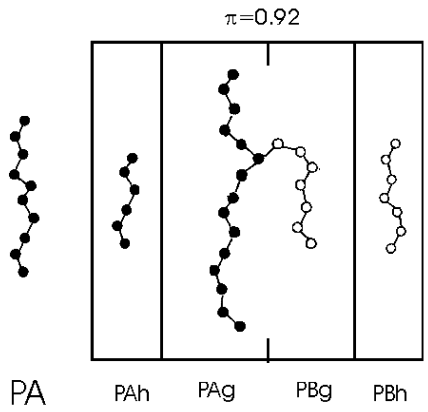

a

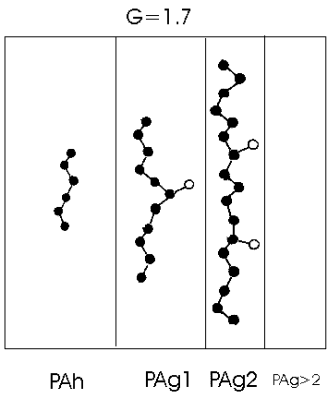

b

Fig. 4. Weight fractions (areas) and molar masses (1 bead ≡ 10 kg/mol) of a mixture PA-h/PB-h/PA-*g*-PB: (a) all components (at the left: PA chains in the feed), (b) PA chains only, classified as to the number of PB-*g* grafts ($g = 0$ for PA-h).

yield an exact picture which must be completed by statistical model calculations. The salient points follow now.

The polymerisation kinetics of free chains PB-h (which can be measured) and those of grafts PB-*g* are similar, and so are normally their molar masses[1] (Eq. (A3)):

$$M_{\mathrm{PBh}} \cong M_{\mathrm{PB}g} \equiv M_{\mathrm{PB}} \tag{4}$$

The polymer PA is less simple. The molar mass of the original PA chains (which can be measured) is not equal to those in the products. The original PA chains are shorter than the grafted PA-*g* chains but longer than the still ungrafted PA-h chains, simply because longer chains are statistically attacked more often by initiator radicals:

$$M_{\mathrm{PAh}} < M_{\mathrm{PA}} < M_{\mathrm{PA}g} \tag{5}$$

The model predicts that, as shown in Fig. 4a, PA-*g* chains are longer than PA-h chains by the factor (Eq. (A6))

$$\frac{M_{\mathrm{PA}g}}{M_{\mathrm{PAh}}} \cong 1 + G \tag{6}$$

Fig. 4a is informative but it does not yet explain salami morphologies. It is important to point out why.

One should think that blends PA-h/PB-h/PA-*g*-PB, consisting of two homopolymers and a graft copolymer, behave like homopolymer blends PA/PB/PA-*b*-PB with a block copolymer. The phase effects in such blends are well known [23–30]: if the block copolymer PA-*b*-PB is asymmetric, with a long PA-b and a short PB-b block, it is interface inactive, forming micelles in the PA phase. However, if its blocks are of similar lengths, it is interface active and concentrates in monolayers between the PA and PB phases. If the copolymer chains PA-*b*-PB are too short, shorter than those of the homopolymers PA and PB, the copolymer can even form a separate phase. A block copolymer PA-*b*-PB thus can change the morphology of a blend considerably. However, it will never build up cellular salami domains as in Fig. 1.

Neither should a graft copolymer PA-*g*-PB. Yet it does, due to a difference between block and graft copolymers that is usually overlooked: anionically made block copolymers have an exact number of blocks, normally two or three when used as blend additives. However, radically made graft copolymers PA-*g*-PB are always mixtures of chains differing in the number of grafts. In other terms, adding a graft copolymer to a blend is equivalent to adding several block copolymers differing the number of blocks and the block length ratio.

The situation at the point of matrix inversion is shown by Fig. 4b. At the conversion $\pi = 0.92$ where the average number of grafts is $G = 1.7$, most PA chains carry no (PA-h), one (PA-*g*-PB_1) or two (PA-*g*-PB_2) grafts. The fractions are given by (Eq. (A8))

$$g = 0: \quad f_{\mathrm{PAh}} = \frac{w_{\mathrm{PAh}}}{w_{\mathrm{PA}}} = \frac{1}{G^2} \tag{7}$$

$$g = i: \quad f_{\mathrm{PA}g=i} \cong i\frac{G-1}{G} f_{\mathrm{PAh}}$$

This distribution is the basis of the model for salami domains in Ref. [22] where it was demonstrated (for a HIPS system) that the chains PA-*g*-PB_2 with two grafts were interface active while the chains PA-*g*-PB_1 with one graft were not.

The reasons are the same as those explained above for the block copolymers: the graft copolymer PA-*g*-PB_1 is interface inactive since it is asymmetric, having a long backbone PA-*g* and a shorter graft PB-*g*, and it is overall fairly short-chained. It feels more at ease forming micelles inside the PA-h phase. On the contrary, the copolymer PA-*g*-PB_2 is interface active and will form monolayers between PA-h and PB-h because it contains PA-*g* and PB-*g* in similar shares and is overall much longer-chained (Fig. 4).

[1] All molar masses and other parameters are number averages.

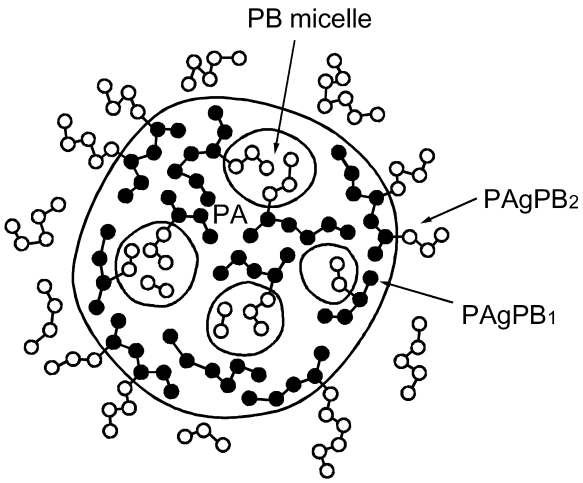

Fig. 5. Salami domain of PA (black) in a PB (white) matrix, with graft copolymer chains PA-*g*-PB_2 in the surface and PA-*g*-PB_1 around the subdomains.

The balance of PB-*g* and PA-*g* in chains PA-*g*-PB_i with $g = i$ grafts is given by (Eq. (A7))

$$x_{g=i} = \frac{M_{PBg=i}}{M_{PAg=i}} \cong \frac{i}{1+i} G \frac{M_{PB}}{M_{PA}} \tag{8}$$

and the total molar mass of these chains by (Eq. (A9))

$$M_{PAg=iPB} = M_{PAg=i} + iM_{PBg=i} = \frac{1+i}{G} M_{PA} + iM_{PB} \tag{9}$$

The differences between PA-*g*-PB_1 and PA-*g*-PB_2 are obvious in Fig. 4b. In blends, the two copolymers behave differently as shown in Fig. 5 where a salami domain is shown in a PB-h matrix [22]. Of the two graft copolymers,

- the interface active PA-*g*-PB_2 forms a monolayer on the domain surface, between the PA-h and PB-h phase, thus stabilizing the domain, while
- the interface inactive PA-*g*-PB_1 forms micelles inside the domain, thus providing the salami substructure.

Therefore, products of grafting-from processes as in Fig. 4, at their inversion point, should be referred to as quaternary blends PA-h/PB-h/PA-*g*-PB_1/PA-*g*-PB_2 with two graft copolymers. This model was developed on HIPS data but the following sections will demonstrate that it describes graft copolymerisations in solutions EP/MMA as well.

3. Experimental

The poly(ethylene-*co*-propylene-*co*-2-ethylidenenorbonene) (EP) was Keltan 314 (DSM). It consisted of the counits 1,4-*cis*, 1,4-*trans* and 1,2 in the weight ratio 50:42:8, had a molar mass of $M_n = 95$ kg/mol ($M_w/M_n = 2.6$) and a glass transition temperature of $T_g = -46$ °C.

Feeds EP/MMA for the grafting-from reactions will be characterized by (*R*,*L*), where *R* is the MMA:EP weight ratio (Eq. (1)) and *L* the volume-weight ratio of the solvent toluene and EP:

$$R = \frac{m_{MMA}}{m_{EP}}, \qquad L = \frac{V_{solv}}{m_{EP}} \tag{10}$$

The following recipe is written for the particularly successful combination ($R = 3$, $L = 8$). In a 250 ml reactor with an anchor stirrer, reflux condenser and nitrogen protection, 15 g EP were dissolved at 75 °C in 120 ml toluene, then 45 g MMA were added together with 150 mg of the initiator benzoyl peroxide (BPO). Polymerisation caused almost immediately clouding of the initially clear

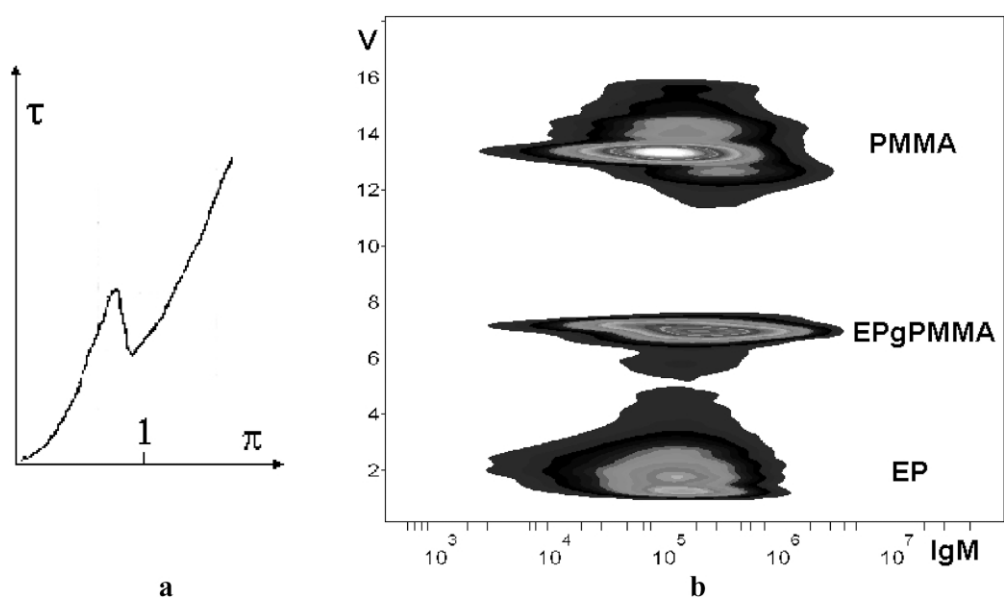

Fig. 6. Graft copolymerisation: (a) stirrer torque τ (as a measure of the viscosity) with a peak at the matrix inversion, (b) two-dimensional chromatography of the product at $\pi = 1.70$, *M*: molar mass, *V*: elution volume in a gradient from isooctane to THF (see Ref. [32]).

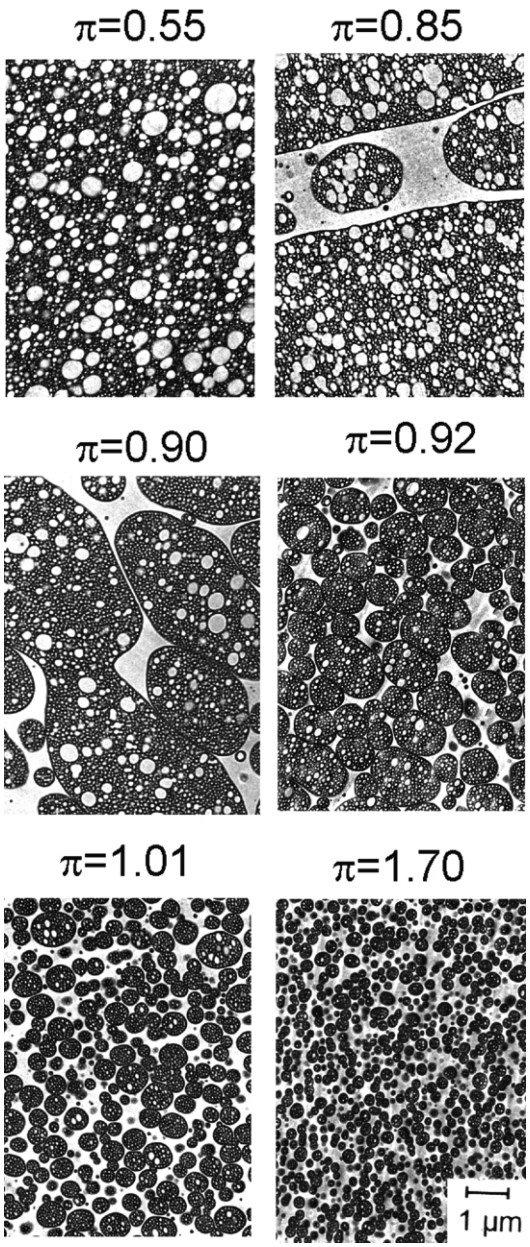

Fig. 7. Evolution of morphologies during grafting-from of the feed EP/MMA$_{R=3,L=8}$ as a function of the conversion π (contrast: EP black, PMMA white).

solution. The torque on the stirrer increases usually steadily but the matrix inversion at $\pi \cong 1$ causes a dip (Fig. 6a) [31].

Samples were taken during the process for determining the composition of the mixture and the phase morphology. One part of these samples was precipitated in methanol, to measure the conversion π (Eq. (1)) gravimetrically and by ^{1}H NMR spectroscopy, another part was dried to obtain samples for transmission electron microscopy (TEM). TEM pictures were taken from ultrathin sections stained with OsO_4. From the precipitated samples, PMMA was extracted with acetone–ethanol. These samples were also redissolved for GPC coupled with gradient chromatography in a solvent gradient ranging from pure isooctane to pure THF as outlined in Ref. [32].

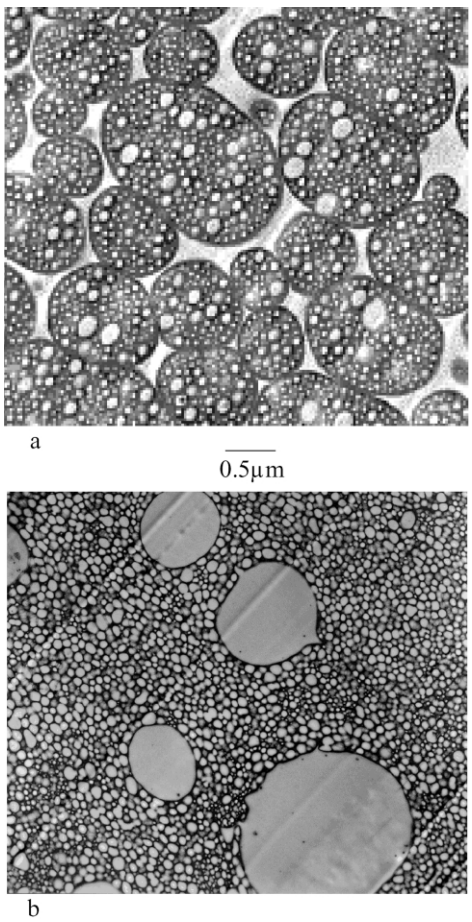

Fig. 8. System EPh/PMMAh/EP*g*PMMA just after the matrix inversion ($\pi = 0.92$): (a) in situ salami morphology (magnification from Fig. 7), (b) the same sample after dissolution in toluene and film casting: PMMAh domains in a EP matrix (small micelles in the EP matrix: EPgPMMA$_1$, monolayers around PMMAh domains: EPgPMMA$_2$).

4. Results

The feed solutions EP/MMA in this study contain more polymer than in industry. The polymer–monomer weight ratio is low, $R \geq 2$, too, much lower than feed solutions for HIPS ($R \cong 8$). Dilution of these mixtures with toluene was necessary to keep the viscosity in limits. The EP/MMA feeds are therefore characterized by R and L (Eq. (10)).

Grafting-from in the system EP/MMA$_{R=3,L=8}$ yielded the morphologies in Fig. 7. The matrix inversion is a sudden transition. At $\pi = 0.85$, the matrix is still EP but the system is already cocontinuous at $\pi = 0.90$ and the matrix changes to PMMA at $\pi = 0.92$ where salami domains appear with diameters on the micrometer scale. At $\pi \geq 1$, these domains decrease in size, eventually down to the stage of graft copolymer micelles (which was not quite reached at $\pi = 1.70$).

The newly born salami domains are shown again in Fig. 8a. The matrix is PMMA, but the concentration of the salami domains is so high that they touch. It is the salami phase, not the PMMA matrix phase, which is in

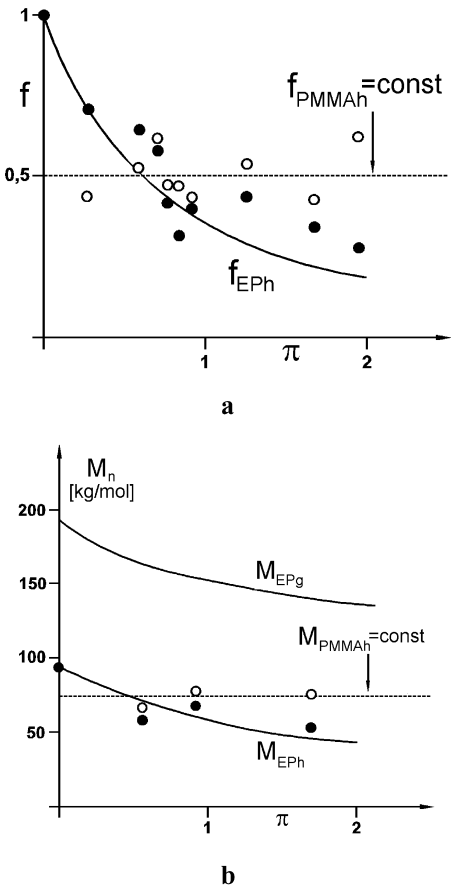

Fig. 9. Data and calculation: (a) shares f_{EPh} and f_{PMMAh} of the ungrafted homopolymers EPh and PMMAh, curve for f_{EPh} with Eq. (A8), $g = 0$, (b) molar masses of the grafted (M_{EPg}) and ungrafted EP (M_{EPh}) and the ungrafted PMMAh (M_{PMMAh}), curves for M_{EPg} and M_{EPh} with Eq. (A6).

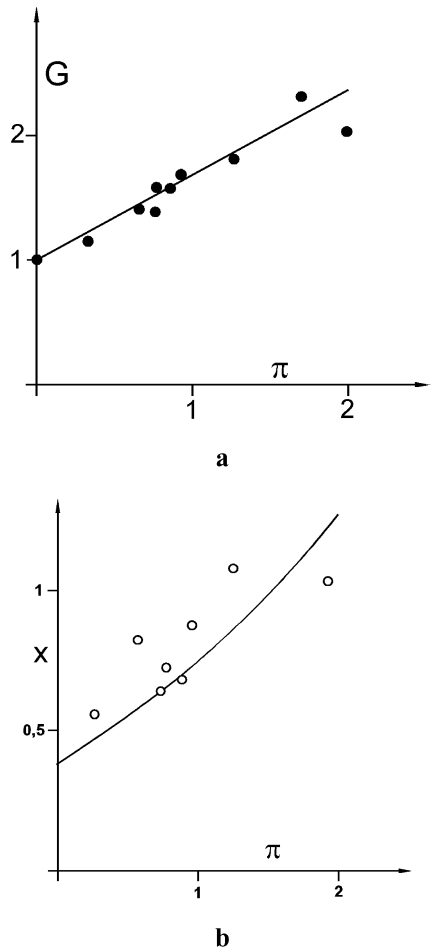

Fig. 10. Composition of the graft copolymer EP*g*PMMA, data and calculation: (a) number of grafts per chain G, curve with Eq. (A5), (b) PMMA*g*–Ep*g* weight balance x, curve with Eq. (A7).

this stage by volume the major phase. Therefore, when this structure is redissolved in toluene and a film is cast, the structure in Fig. 8b results, which is reinverted: the matrix is again EP. The film structure in Fig. 8b is thermodynamically controlled while the inverted salami morphology in Fig. 8a results from efficient stirring. It is this effect of technology that gave these products the name of *products by process*.

The model for salami domains in Fig. 5 is well supported by Fig. 8, together with Fig. 4 which refers to the same system.[2] As demonstrated in Fig. 8b, the majority of the graft copolymer chains form micelles in the EPh phase. These are the surface inactive copolymer chains EP*g*PMMA$_1$ (Fig. 4b). They form the same micelles inside the salami domains in Fig. 8a.

The surface active chains EP*g*PMMA$_2$, of which there are less (Fig. 4b), form in Fig. 8b monolayers around the PMMAh domains. They stabilize in Fig. 8a the salami domains, forming a surface layer that keeps these domains from coalescing although they touch each other.

As the polymerisation goes on, after the matrix inversion, EP becomes more and more grafted. The ungrafted polymers EPh and PMMAh are characterized in Fig. 9 by the fractions f_{EPh} and f_{PMMAh} and the molar masses M_{EPh} and M_{PMMAh}. As expected, the values for PMMAh are constants, $f_{PMMAh} = 0.5$ and $M_{PMMAh} = 72$ kg/mol. These two parameters, together with the conversion π and the molar mass $M_{EP} = 95$ kg/mol of the original EP, were used to calculate the curves in Figs. 9 and 10 from the statistical equations.

The data in Fig. 9 confirm that f_{EPh} and M_{EPh} decrease steadily. Of course, the M_{EPg} curve for the EP*g* backbones of graft copolymer chains EP*g*PMMA cannot be compared with experimental data. According to the calculation, the grafted backbones EP*g* are very long indeed. The model predicts that the first backbones EP*g* to be grafted are on average twice as long as the original EP chains (Eq. (A6)). The graft copolymer EP$_{1-x}$*g*PMMA$_x$ is characterized in Fig. 10 by the number of

[2] PA = EP and PB = PMMA in Fig. 4 (ungrafted EPh is classified as a homopolymer).

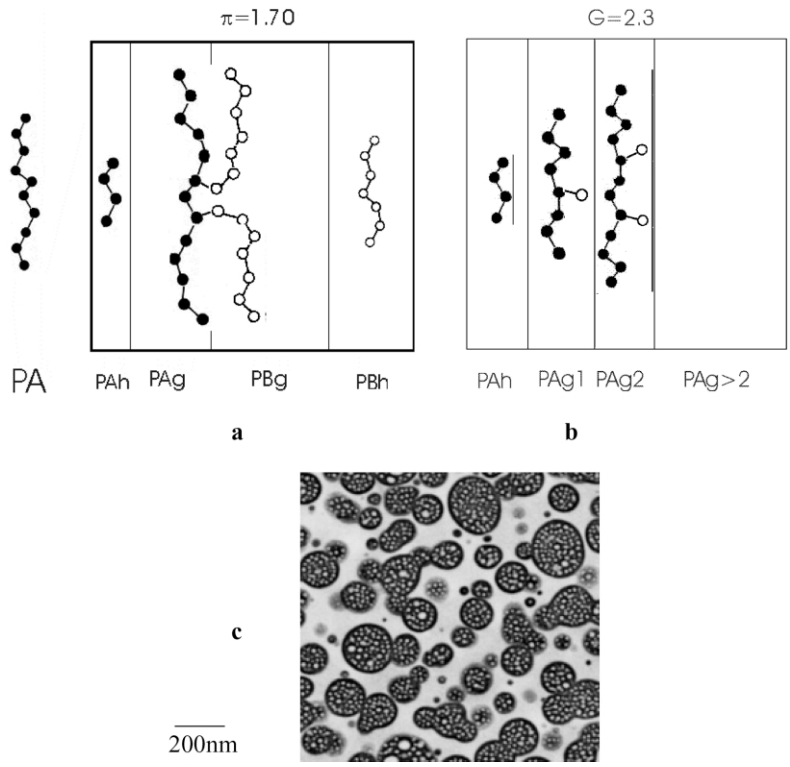

Fig. 11. Late stage of grafting-from ($\pi = 1.70$): (a), (b) composition (as Fig. 4), (c) structure of small salami domains (magnification from Fig. 7).

grafts G and the composition x. The model equations do fairly well.

Diagrams as in Fig. 4 are shown in Fig. 11a and b for a late stage ($\pi = 1.7$). The increase of grafting is obvious. The shift towards highly grafted EP*g*PMMA chains ($PA_{g>2}$) causes the salami domains to shrink. The big domains break apart since more and more copolymer chains prefer the domain surface and less the interior (Fig. 11c, compare with Fig. 8a). The decrease in domain size due to ongoing grafting is shown in Fig. 12.

This effect of domain size decrease can be and is, in industry, avoided: if stirring is discontinued, after the matrix inversion, the salami domains do not shrink in size. Instead, they swell, and their internal subdomains grow. Comparison of Figs. 1 and 8a demonstrates this: the HIPS structure in Fig. 1 is an end product with big, swollen subdomains, while Fig. 8a shows the domains at birth, with a substructure of tiny micelles. This effect of domain swelling after the matrix inversion is the topic of the second part of this report.

So far, only a run EP/MMA with the feed ($R = 3$, $L = 8$) was discussed. Changing the feed composition (R,L) leads to salami domains only at the points shown

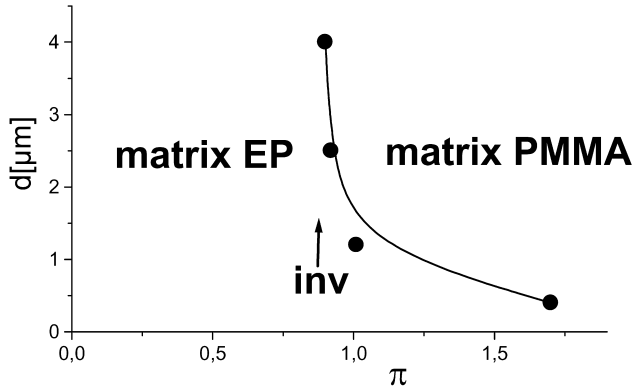

Fig. 12. Average diameter of the salami domains after the matrix inversion (inv).

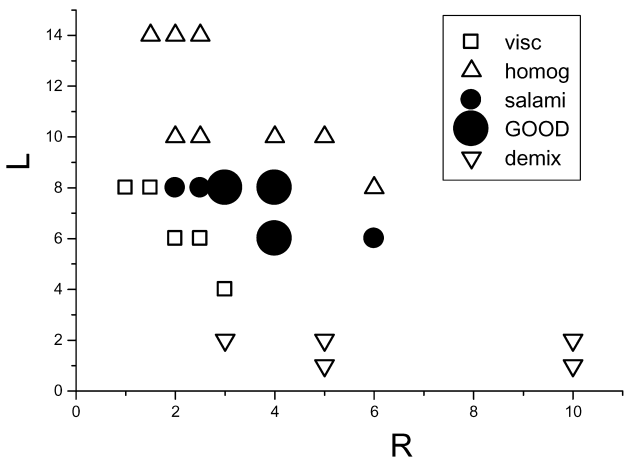

Fig. 13. Morphology map of systems (R,L) at the point of matrix inversion: some systems are demixed from the start, others remains always homogeneous, still others become too viscous, black dots: salami structures (big dots:good structures).

in Fig. 13. The other composition does not satisfy the conditions. Systems with too much solvent and MMA not phase separate, those with too little solvent and MMA become too viscous, and those with too little toluene are demixed from the start. For salami domains, the recipe ($R = 3$, $L = 8$) is an optimum.

Acknowledgements

Financial support by the Bundesminister für Wirtschaft through the Arbeitsgemeinschaft Industrieller Forschungsvereinigungen (AiF, Nr.12375) is gratefully acknowledged.

Appendix A. Statistics

Statistically, a mixture PA-h/PB-h/PA-*g*-PB is described by three probabilities, i.e. the probabilities that a A unit is a chain end (α) or a graft point (γ) and the probability that a B unit is a chain end (β).

The distribution of PA chains consisting of a units and carrying g grafts is given by n_{ag} which is a product of two probabilities

$$n_{ag} = n_a n_g,$$

$$n_a = \frac{\alpha}{1-\alpha}(1-\alpha)^a, \qquad n_g = (a,g)\left(\frac{\gamma}{1-\gamma}\right)^g (1-\gamma)^a \tag{A1}$$

while the distribution of PB chains having b units is given by

$$n_b = \frac{\beta}{1-\beta}(1-\beta)^b \tag{A2}$$

The probabilities α, β and γ can be determined by measuring four experimental parameters, normally the molar mass M_{PA} of the original PA chains in the feed and the conversion π of the polymerisation as well as the fraction f_{PBh} and the molar mass M_{PBh} of the extracted PB-h:

$$M_{PA} = \frac{M_A}{\alpha} = \frac{G^*}{\gamma} M_A,$$
$$M_{PBh} \cong M_{PBg} \cong M_{PB} = \frac{M_B}{\beta} \tag{A3}$$

where M_A and M_B are the monomer molar masses and G^* is the number of PB-*g* grafts per PA chain, given by

$$G^* = \frac{w_{PBg}}{w_{PA}} \frac{M_{PA}}{M_{PB}} = \sum_{a=1}^{\infty}\sum_{g=0}^{\infty} g n_{ag} = (1 - f_{PBh}) \frac{M_{PA}}{M_{PB}} \pi \tag{A4}$$

This number G^* includes ungrafted PA chains (PA-h) as well. If those are excluded, the number of PB-*g* grafts per PA-*g* chain is (Eq. (3)):

$$G = \sum_{a=1}^{\infty}\sum_{g=1}^{\infty} g n_{ag} = \frac{1-(1-\alpha)(1-\gamma)}{\alpha} \cong 1 + G^* \tag{A5}$$

The molar masses M_{PAh} of the ungrafted and M_{PAg} of the grafted PA chains (Eq. (6)) can be calculated from

$$M_{PAh} = M_A \frac{\sum_{a=1}^{\infty} a n_a n_{g=0}}{\sum_{a=1}^{\infty} n_a n_{g=0}} = \frac{M_{PA}}{G},$$

$$M_{PAg} = M_A \frac{\sum_{a=1}^{\infty}\sum_{g=1}^{\infty} a n_a n_g}{\sum_{a=1}^{\infty}\sum_{g=1}^{\infty} n_a n_g} \tag{A6}$$

$$= \frac{M_A}{\alpha} \frac{1-(1-\alpha)^2(1-\gamma)}{1-(1-\alpha)(1-\gamma)} \cong \left(1 + \frac{1}{G}\right) M_{PA}$$

and the composition x of the graft copolymer $PA_{1-x}g\,PB_x$ (Eq. (2)) from

$$x = \frac{G M_{PBg}}{M_{PAg}} = \frac{G^2}{1+G} \frac{M_{PB}}{M_{PA}} \tag{A7}$$

Chains $PA_{g=i}$ with a specific number $g = i$ of grafts are described by Eqs. (7)–(9). Their shares and molar masses are

$$f_{PAg=i} = \frac{\sum_{a=1}^{\infty} a n_a n_g}{\sum_{a=1}^{\infty} a n_a} \cong \frac{i+1}{G^2}\left(1 - \frac{1}{G}\right)^i \tag{A8}$$

$$M_{PAg=i} = M_A \frac{\sum_{a=1}^{\infty} a n_{ag}}{\sum_{a=1}^{\infty} n_{ag}} = \frac{1+i}{G} M_{PA} \tag{A9}$$

References

[1] Echte A. Angew Makromol Chem 1977;58/59:175.
[2] Echte A. Adv Chem Ser 1989;222:15.
[3] Keskkula H. Plast Rubber Mater Appl 1979;16:56.
[4] Echte A, Gausepohl H, Lütje H. Angew Makromol Chem 1980;90:95.
[5] Echte A, Haaf F, Hambrecht J. Angew Makromol Chem 1981;93:372.
[6] Haaf F, Breuer H, Echte A, Schmidt BJ, Stabenow J. J Sci Ind Res 1981;40:659.
[7] Bucknall CB. Toughened plastics. London: Applied Science Publishers; 1979.
[8] Bucknall CB. In Paul DR, Bucknall CB, editors. Polymer blends, vol. II. New York:Wiley;1999. p. 83, Chapter 22.
[9] Michler GH. Kunststoff-Mikromechanik. Munich: Hanser; 1992. chapters 7.2 and 9.2.
[10] Bucknall CB, Karpodinis AM, Zhang XC. J Mater Sci 1994;29:3377.
[11] Lazzeri A, Bucknall CB. Polymer 1995;36:2895.
[12] Molau GE, Keskkula H. J Polym Sci A1 1966;4:1595.

[13] Brydon A, Burnett GM, Cameron GG. J Polym Sci, Polym Chem Ed 1973;11:3255.
[14] Fischer JP. Angew Makromol Chem 1973;33:35.
[15] Severini F, Pegoraro M, di Landro L. Angew Makromol Chem 1991; 190:177.
[16] Liu NC, Baker WE. Adv Polym Technol 1992;11:249.
[17] Collyer AA. Rubber toughened engineering plastics. London: Chapman & Hall; 1994.
[18] Falk JC, van Fleet J, Rasmussen J. Angew Makromol Chem 1977;57: 77.
[19] Shaw S, Singh RP. J Appl Polym Sci 1990;40:701.
[20] Park DJ, Ha CS, Cho WJ. J Appl Polym Sci 1994;54:763.
[21] Hellmann GP, Walter M, Dietz M, Steurer A. Macromol Symp 1996; 112:175.
[22] Fischer M, Hellmann GP. Macromolecules 1996;29:2498.
[23] Hudson, S.D., Jamieson, A.M., in DR Paul, Bucknall CB, editors. Polymer blends, vol. I. New York:Wiley;1999. p. 461, Chapter 15.
[24] Adedeji A, Hudson SD, Jamieson AM. Macromolecules 1995;28: 5255.
[25] Adedeji A, Hudson SD, Jamieson AM. Macromolecules 1996;29: 2449.
[26] Adedeji A, Hudson SD, Jamieson AM. Macromol Chem Phys 1996; 197:2521.
[27] Löwenhaupt B, Hellmann GP. Colloid Polym Sci 1990;268:885.
[28] Löwenhaupt B, Hellmann GP. Colloid Polym Sci 1994;272:121.
[29] Löwenhaupt B, Hellmann GP. Polymer 1991;32:1065.
[30] Löwenhaupt B, Steurer A, Hellmann GP, Gallot Y. Macromolecules 1994;27:908.
[31] Freeguard GF, Karmarkar M. J Appl Polym Sci 1971;15:1649.
[32] Siewing A, Schierholz JU, Braun D, Hellmann GP, Pasch H. Macromol Chem Phys 2001;202:2890.